Effects of Thickness Extension Mode Resonance Oscillation of Acoustic Waves on Catalytic and Surface Properties I. Ethanol Decomposition on a Thin Ag Film Catalyst Deposited on Positively Polarized Z-Cut $LiNbO_3$

N. Saito and Y. Inoue*

Department of Chemistry, Nagaoka University of Technology, Nagaoka 940-2188, Japan

Received: November 14, 2001; In Final Form: March 5, 2002

A 100-nm thick Ag film was deposited on a positively polarized z-cut $LiNbO_3$ ferroelectric substrate, and the effects of thickness extension mode resonance oscillation (TERO) of bulk acoustic waves generated by rf electric power on the catalytic properties were studied. In ethanol decomposition, the TERO caused a remarkable increase in ethylene production without changes in acetaldehyde production, and the activation energy for ethylene production decreased considerably. The activity for ethylene production increased in a nonlinear manner with increasing rf power, and its selectivity resulted in a marked enhancement. A laser Doppler method demonstrated that the TERO produced randomly distributed standing waves with large lattice displacement vertical to the surface. In photoelectron emission spectra, the TERO caused a positive shift of the threshold energy in photoelectron emission from the Ag surface, which was indicative of an increase in a work function-related parameter in the presence of TERO. The vertical dynamic lattice displacement is proposed to be responsible for positive work function shifts. Correlation existed between activity enhancement and the work function shift, which indicated that activity enhancements with TERO are associated with increases in the work function. A mechanism of TERO effects on selectivity changes is discussed.

Introduction

In a study of acoustic wave effects on heterogeneous catalysis, surface acoustic waves (SAWs) and the resonance oscillation (RO) of bulk acoustic waves generated by applying radio frequency (rf) electric power to poled ferroelectric substrates have been used. For the SAWs, thin film metal and metal oxide catalysts were deposited on the propagation path of the SAWs between two interdigital transducer electrodes fabricated on the same plane of the ferroelectric substrates.[1−6] For the RO, the catalysts were deposited on the front and back planes of the ferroelectric substrates.[7−15]

In a previous study of RO effects on catalysis, thickness extension mode resonance oscillation (TERO) generated on a z-cut $LiNbO_3$ single crystal substrate has been found to enhance ethylene production without a change in acetaldehyde production in ethanol decomposition on a Ag catalyst, exhibiting the ability of TERO to increase ethylene production selectively.[9,11,13] Furthermore, it was shown that thickness shear mode resonance oscillation (TSRO) generated on an x-cut $LiNbO_3$ single-crystal substrate caused no activity enhancement for both ethylene and acetaldehyde production.[9] The analysis of the vibrational modes by a laser Doppler method demonstrated that lattice displacement of the TERO was vertical to the surface, whereas that of the TSRO was parallel to the surface.[9,11] Thus, the interesting findings are that selectivity changes were induced in a case in which acoustic wave-induced lattice displacement was vertical to the catalyst surface.

A z-cut $LiNbO_3$ ferroelectric substrate employed for TERO has spontaneous polarization perpendicular to the surface, which means that the crystal exposes a positively polarized plane at one side and a negatively polarized plane at the other. A previous study was performed on the Ag catalysts deposited on the negatively and positively polarized surfaces; the results obtained involved both contributions from the oppositely polarized surfaces.[9,11,13] For a better understanding of the mechanism of acoustic wave excitation, it is important to clarify each role of the polarized substrate surfaces in the TERO effects that are able to control the catalytic selectivity. In the present study, therefore, a catalyst is designed to have a thin Ag film on a positively polarized plane of z-cut $LiNbO_3$, whereas a negatively polarized plane is covered with a catalytically inactive thin Au film so as to avoid its contribution to the TERO effects.

The kinetic behavior of ethanol decomposition was investigated in the absence and presence of TERO and was compared with the previous results for a Ag catalyst deposited on both positively and negatively polarized substrates. Lattice displacement caused by TERO was analyzed in detail by means of a 3-D laser Doppler method. To obtain information on changes in the electronic structures with RO effects, photoelectron emission spectroscopic measurements were employed for TERO and TSRO, and the threshold energy for photoelectron emission was compared between them.

Experimental Section

A poled ferroelectric single crystal of z-cut $LiNbO_3$ (referred to as z-LN) was cut in a rectangular shape of 14 mm in length and 44 mm in width. A catalytically active Ag film (which worked as both an electrode and a catalyst) was deposited at a thickness of 100 nm on a positively polarized substrate surface of the crystal by the resistance heating of pure Ag in a vacuum, whereas the back plane of the negatively polarized surface was covered with a thin Au film that was used as an electrode. The catalyst is denoted here as (+)Ag. The catalytic activity of the

* Corresponding author. E-mail: inoue@analysis.nagaokaut.ac.jp.

10.1021/jp014209q CCC: $22.00
Published on Web 04/18/2002

Au electrode was smaller by a factor of 30 and the activity increase with TERO was lower by a factor of 160 than those of the Ag catalyst. Thus, because of extremely small influences, the Au electrode was regarded as being catalytically inactive.

The resonance frequencies of TERO appeared at 3.5, 10.5, 17.4, and 24.1 MHz, which were consistent with a series of $3.7 \times (2n - 1)$ frequencies, where $n = 1$, 2, 3, or 4, calculated on the basis of a piezoelectric equation.[16,17]

The catalytic ethanol decomposition was carried out in a gas-circulating vacuum apparatus, and reactants and products were analyzed by an on-line gas chromatograph. Selectivity for ethylene production was defined as the amount of ethylene as a percentage of the total amount of ethylene and acetaldehyde production. For the generation of TERO, an rf electric signal from a network analyzer (Anritsu MS3606B) was amplified-(Kalmus, 250FC) and applied to a catalyst after impedance adjustment. In the present work, a primary resonance frequency of 3.5 MHz was used unless otherwise specified. The temperature of the catalyst surface was monitored by shifts in the resonance frequency and kept constant in the absence and presence of TERO by using an outer electric furnace as described elsewhere.[13]

Lattice displacement with TERO was measured using a homemade laser Doppler apparatus.[13] A Ag catalyst surface was irradiated by a He−Ne laser beam, and a reflected beam was monitored by a vibrometer (Ono Sokki LV-1300). A sample stage was moved along the x and y directions while the beam spot was fixed. A 3-D image in the $x-y-z$ direction was obtained as a pattern, and the distribution of lattice displacements as a function of rf power was investigated.

Photoelectron emission from a Ag surface upon UV light irradiation was measured in air by a low-energy photoelectron spectroscopic method.[8] Monochromatized light from a deuterium lamp used to irradiate the Ag surface was scanned over a wavelength range of 230−320 nm. Emitted photoelectrons were counted and plotted against photon energy, and the threshold energy for photoelectron emission corresponding to the work function was compared in the absence and presence of TERO.

Additionally, a thin Ag film catalyst was deposited on an x-cut $LiNbO_3$ substrate that was able to generate TSRO. The effects of TSRO on lattice displacement and the photoelectron emission spectra were investigated and compared with TERO effects.

Results

In ethanol decomposition on a Ag catalyst, both ethylene and acetaldehyde were produced in the gas phase and increased nearly proportionally to the reaction time. When TERO was generated, an immediate increase in ethylene production occurred without a significant enhancement of acetaldehyde production. Figure 1 shows changes in the catalytic activity of ethylene and acetaldehyde with TERO-on and -off. The activity for ethylene production increased 7-fold with TERO-on at a power of 3 W, whereas that for acetaldehyde remained nearly unchanged. Turning the power off resulted in a decrease in the activity to the original low level. Figure 2 shows the temperature dependence of the reaction in the temperature range 573−653 K. Under the TERO-off conditions, the activation energy was 156 kJ mol^{-1} for ethylene and 95 kJ mol^{-1} for acetaldehyde production. With TERO-on, the activation energy of ethylene decreased to 103 kJ mol^{-1}, whereas that for acetaldehyde remained unchanged.

Figure 3 shows the pressure dependence of the reaction. In the absence of TERO, the reaction order, n, with respect to ethanol pressure, P_e, was zero for both ethylene and acetaldehyde production. With TERO-on at 3 W, no significant changes in their pressure dependences occurred; the reaction orders remained zero order.

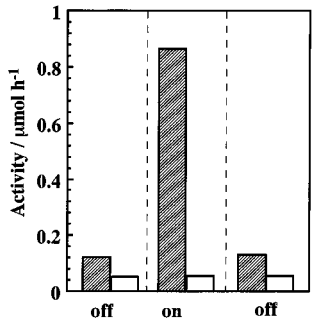

Figure 1. Changes in catalytic activity for ethanol decomposition with TERO-on and TERO-off. (hatched rectangles), ethylene production; (open rectangles), acetaldehyde production; rf power $J = 3$ W; reaction temperature $T_r = 573$ K; ethanol pressure, $P_e = 4.0$ kPa.

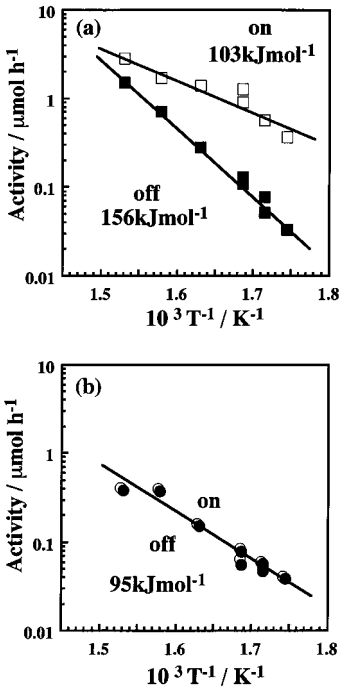

Figure 2. Temperature dependence of ethylene (a) and acetaldehyde (b) production in ethanol decomposition with TERO-off (■, ●) and TERO-on (□, ○). $J = 3$ W, $P_e = 4.0$ kPa.

Figure 4 shows the activity for ethylene and acetaldehyde production as a function of rf power to generate TERO. The activity for ethylene production gradually increased with increasing power followed by a steep rise in a larger power range above 3 W, whereas that for acetaldehyde production remained within a small increase even for rf power greater than 4 W. The selectivity for ethylene production was 45% with TERO-off and increased to 90% at 5 W.

Figure 5 shows the TERO-induced 3-D images of lattice vibration along a direction vertical to a Ag surface. For 1−3 W, standing waves were randomly distributed over the $x-y$ planes. The top-to-bottom distance of the standing waves along the z direction corresponds to lattice displacement that increased remarkably with increasing rf power. Figure 6 shows the distributions of lattice displacement at different power levels. At 1 W, the maximum lattice displacement, L_{max}, was 38 nm, and the average lattice displacement, L_{av}, was 12 nm. The peak of the lattice displacement distribution appeared at 7 nm, and

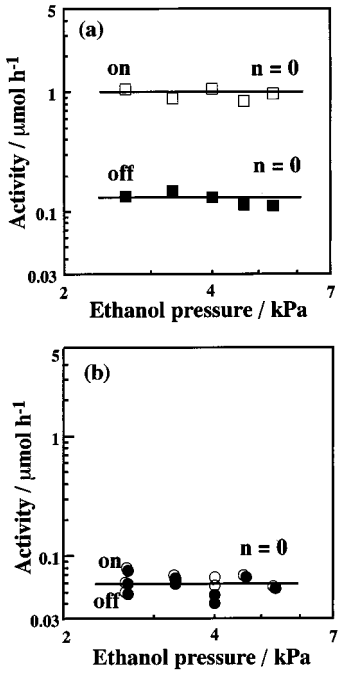

Figure 3. Pressure dependence of ethylene (a) and acetaldehyde (b) production in ethanol decomposition with TERO-off (■, ●) and TERO-on (□, ○). $J = 3$ W, $T_r = 593$ K.

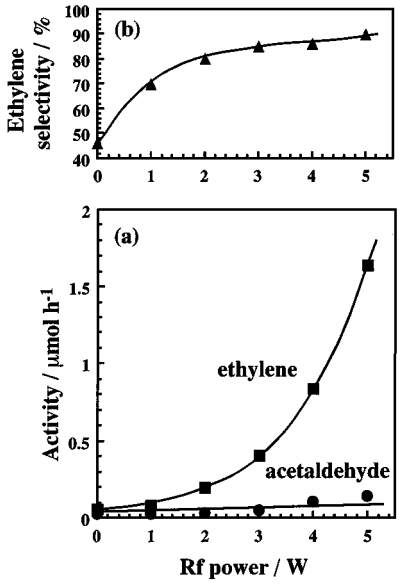

Figure 4. Catalytic activity and selectivity as a function of rf power. ■, activity for ethylene production; ●, activity for acetaldehyde production; ▲, selectivity for ethylene production. $T_r = 593$ K, $P_e = 4.0$ kPa.

the value of the full width at half-maximum (fwhm) was 13 nm. At 2 W, L_{max} and L_{av} increased to 48 and 18 nm, respectively. The lattice displacement distribution became broader: fwhm was 19 nm. The peak maximum of the lattice displacement distribution was 9 nm. At 3 W, L_{max} was attained at 63 nm, and L_{av} was 21 nm. The fwhm was as broad as 22 nm. Figure 7 shows L_{max} and L_{av} as functions of rf power. Both lattice displacements increased significantly in a low power range, followed by a gradual increase with increasing power.

Figure 8 shows the spectra of photoelectron emission from a Ag surface. Photoelectron emission was negligible below a photon energy of 4.40 eV. With TERO-off, the emission occurred at 4.45 eV, and the number of electrons emitted

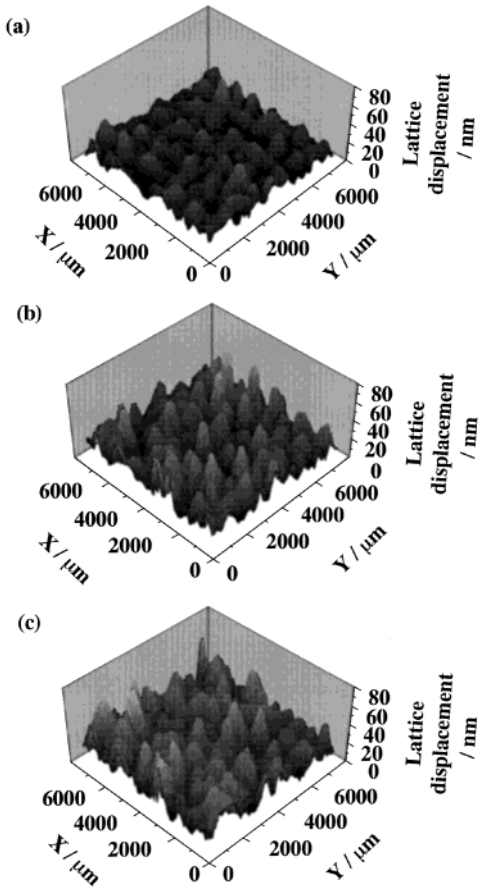

Figure 5. Three-dimensional images of lattice displacement obtained by laser Doppler measurements. (a) $J = 1$ W, (b) $J = 2$ W, (c) $J = 3$ W. Temperature of measurements T_m = room temperature

increased linearly with increasing photon energy, indicating that the threshold energy, Φ, at which electron emission started was 4.45 eV. With TERO-on at 1 W, the electron emission pattern was nearly the same as that with TERO-off within an error of measurement accuracy of <0.02 eV. At 2 W, however, the pattern considerably shifted toward higher photon energy, and the threshold energy increased by 0.09 eV. At 3 W, another shift occurred, and the threshold energy increased by as much as 0.16 eV.

For comparison, photoelectron emission measurements were performed for a Ag surface with TSRO. As shown in Figure 9, no significant threshold energy shift occurred with TSRO on, even at a high rf power of 3 W. Figure 10 shows the shifts of threshold energy as a function of rf power. With increasing rf power, TERO caused a significant positive shift in the threshold energy, whereas TSRO brought about a small shift. It should be noted that there exists an intrinsic difference in the threshold energy shift between TERO and TSRO.

Figure 11 shows the activity enhancements for ethylene production and the threshold energy shifts as a function of maximum lattice displacement, L_{max}. Their changes were small in a low regime of lattice displacement, followed by steep increases above 40 nm. Thus, the striking feature is that both the activity and work functions varied in a similar manner with respect to lattice displacement.

Discussion

TERO-on for (+)Ag caused a dramatic increase in the catalytic activity for ethylene production but not for acetaldehyde production, exhibiting a remarkable increase in the selectivity

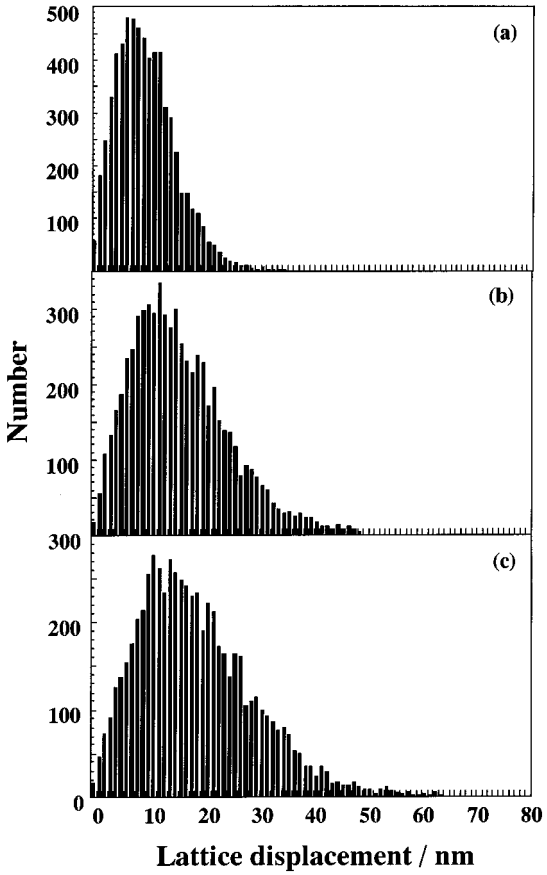

Figure 6. Distributions of lattice displacement as a function of rf power. (a) $J = 1$ W, (b) $J = 2$ W, (c) $J = 3$ W. T_m = room temperature

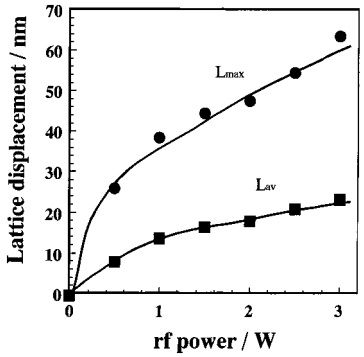

Figure 7. Changes in maximum (L_{max}) and average (L_{av}) lattice displacements with increasing rf power.

for ethylene production. At 3 W, the selectivity increased to 94 from 45%, and the activation energy of the reaction decreased to 103 from 156 kJ mol^{-1} (the extent of decrease was 34%). It is interesting to compare the present results with the previous ones that were obtained for a Ag catalyst deposited on both positively and negatively polarized substrate surfaces (denoted here as (±)Ag). For (±)Ag, the selectivity for ethylene production increased to 90%, and the activation energy decreased to 115 kJ mol^{-1} (the extent of decrease was 26%) under similar reaction and rf power conditions.[13] Thus, the selectivity and activation energy for (+)Ag were slightly larger than those for (±)Ag. These results suggest that the positively polarized substrate induces larger TERO effects than does the negatively polarized substrate.

In the absence of TERO, the reaction order with respect to ethanol pressure was zero. By assuming that the rate-determining step is the decomposition of adsorbed ethanol, the reaction rate, V, is given by

$$V = k\theta = kKP_e/(1 + KP_e) \quad (1)$$

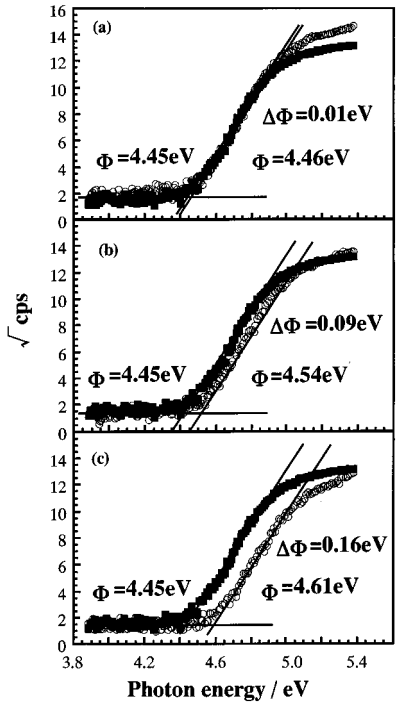

Figure 8. Photoelectron emission spectra of Ag with TERO-off (■) and TERO-on (○). (a) $J = 1$ W, (b) $J = 2$ W, (c) $J = 3$ W. T_m = room temperature.

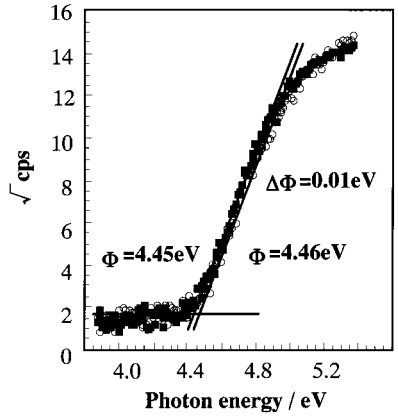

Figure 9. Photoelectron emission spectra of Ag with TSRO-off (■) and TSRO-on (○) at $J = 3$ W. T_m = room temperature.

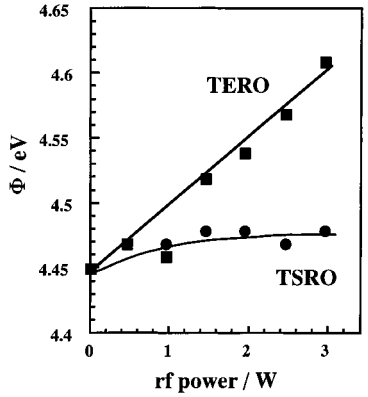

Figure 10. Threshold energy shifts with TERO and TSRO as functions of rf power.

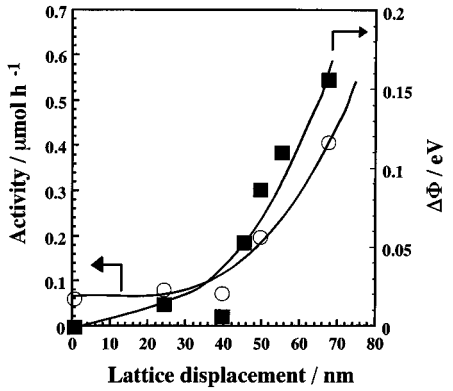

Figure 11. Changes in catalytic activity and shifts of threshold energy with maximum lattice displacement L_{max}. ■, threshold energy shift; ○, catalytic activity for ethylene production.

where k is the rate constant, θ is the surface coverage of ethanol, K is the equilibrium constant of ethanol adsorption, and P_e is the ethanol pressure. Under the conditions of strong adsorption of ethanol at a high ethanol pressure, that is, $1 \ll KP_e$, the equation approximates to $V = k$. Thus, the experimental reaction order suggests that the decomposition of strongly adsorbed and fully surface-covering ethanol is the rate-determining step.

In a previous study of ethanol oxidation over a thin Pd film deposited on positively polarized z-cut $LiNbO_3$, the TERO caused a decrease in activation energy from 156 to 36 kJ mol^{-1}.[14] Furthermore, the TERO increased the reaction order with respect to ethanol pressure from 0.2 to 1.0, thus decreasing the order with respect to oxygen pressure from 0.5 to −0.1. A large increase in the ethanol reaction order indicates that the TERO weakens the adsorption of ethanol in ethanol oxidation over the Pd surface.[14] Although there is a possibility that the adsorption of ethanol on the Ag surface is weakened in a similar manner, little change in the order of the reaction (zeroth order) with respect to ethanol pressure suggests that the catalytic sites of the Ag surface are fully covered with ethanol species even in the presence of the TERO. A significant decrease (from 156 to 103 kJ mol^{-1}) in the activation energy of ethylene production with TERO shows that the TERO is able to reduce the energy barrier of the surface reaction for ethylene production. Thus, it is apparent that the activity enhancement with TERO is related to changes in kinetic factors promoting the abstraction of both H and OH groups from an adsorbed ethanol rather than changes in thermodynamic factors regarding the concentration of ethanol adsorbed on the Ag surface.

As shown in Figure 5, the 3-D images observed in laser Doppler measurements exhibited a variety of standing waves distributed randomly over the Ag surface. The important feature was the presence of a very large displacement vertical to the surface with TERO, which contrasted with a very small vertical component of lattice displacement observed previously for TSRO. Another feature was the considerable differences in the characteristics of lattice displacement between below and above 1 W: the fwhm of the standing waves at 1 W was as narrow as 13 nm, whereas the values at 2 and 3 W were broadened to 19−22 nm. This result indicates that the proportion of large lattice displacements increased remarkably at power higher than 2 W.

The photoelectron emission spectra showed that the TERO caused the shift of the threshold energy toward higher photon energy. Because the threshold energy is associated with the work function, these results are indicative of increases in the work function with TERO. According to a jellium model, the work

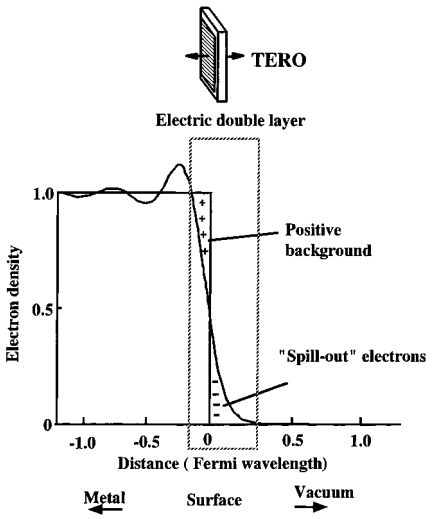

Figure 12. Model of work function changes with TERO-on.

function of a metal is determined by a dipole electric layer and cohesive energy. In transition metals, the former plays an important role. As shown in Figure 12, the dipole electric layer is composed of two charges: one is a negative charge resulting from electrons that spill out from the topmost surface atoms and the other is a positive charge remaining in the interior of the surface.[18,19] Thus, the density of electrons that spill out from the topmost surface is an important factor. If one assumes that the vertical lattice displacement has an influence on the spilled-out electrons, there is the possibility that the density of the electrons changes with the generation of TERO because the direction of lattice displacement is the same as the direction toward which electrons spill from the topmost layer of the surface. This assumption can be verified by the fact that the work function shift occurred only with TERO but not with TSRO, which had no component of lattice displacement vertical to the surface.

On the basis of the rf power dependence, changes in the catalytic activity and in the work function were plotted as functions of lattice displacement, L_{max}. As shown in Figure 11, the catalytic activity and the work function varied in a similar manner with increasing lattice displacement. The close correlation indicates that the work function changes are responsible for the catalyst activation of ethanol decomposition on a Ag catalyst.

For the enhancement of ethylene selectivity with the TERO, one possible mechanism is a change in the adsorbed structure of ethanol. Electron back-donation from a metal surface to an oxygen atom of adsorbed ethanol is impotant for the formation of strongly bonded adsorbed species. Increases in the work function with TERO lower the ability to transfer electrons to the adsorbed species, and hence lead to weak bond formation.[20,21] The weak interaction of ethanol with a metal surface results in the formation of molecularly chemisorbed ethanol, whereas the strong interaction produces ethoxy species by dissociating an OH bond. It is likely that an increase in the work function with TERO converts ethoxy species to molecularly chemisorbed ethanol on the Ag surface. Küppers et al. studied the adsorption and decomposition of ethanol on Ni(100) surfaces using FT-IRAS and showed that the orientation of adsorbed ethanol species to the surface was different depending on the kinds of chemisorbed ethanol[22] that were involved. For molecularly chemisorbed ethanol, its O−H bond was oriented parallel to the surface, whereas an ethoxy species had an orientation with the C−C bond perpendicular to the surface.

The decomposition of the ethoxy species was thought to be followed by the abstraction of an α-hydrogen atom.[22] These results indicate that α-H−C scission occurs with the ethoxy species, whereas the abstraction of the HOH group is favored for molecularly chemisorbed ethanol because the ethanol species has an inclined conformation that permits easier access of β-H and OH groups to the Ag surface. The latter leads to the promotion of ethylene production. This consideration explains the TERO effects that enhance the selectivity for ethylene production.

In conclusion, TERO-on for a (+)Ag catalyst has remarkable effects on selectivity enhancement for ethylene production in ethanol decomposition. The effects are proposed to be mainly due to changes in the electronic structure of the (+)Ag surface that are caused by dynamic vertical lattice displacement. An increase in ethylene selectivity is associated with variations of the adsorbed species. The present results suggest that there are differences in TERO effects between (+)Ag and (−)Ag. In this regard, it is required that the TERO effect of a Ag catalyst deposited on a negatively polarized surface be examined.

Acknowledgment. This work was supported by a Grant-in-Aid for Scientific Research (B) from The Ministry of Education, Science, Sports and Culture. N.S. acknowledges a grant from the Sumitomo Foundation.

References and Notes

(1) Inoue, Y.; Matsukawa, M.; Sato, K. *J. Am. Chem. Soc.* **1989**, *111*, 8965.
(2) Inoue, Y.; Matsukawa, M.; Sato, K. *J. Phys. Chem.* **1992**, *96*, 2222.
(3) Nishiyama, H.; Saito, N.; Shima, M.; Watanabe, Y.; Inoue, Y. *Faraday Discuss. Chem. Soc.* **1997**, *107*, 425.
(4) Kelling, S.; Mitrelias, T.; Matsumoto, Y.; Ostanin, V. P.; King, D. A. *Faraday Discuss. Chem. Soc.* **1997**, *107*, 435.
(5) Kelling, S.; Cerasari, S.; Rotermund, H. H.; Ertl, G.; King, D. A. *Chem. Phys. Lett.* **1998**, *293*, 325.
(6) Nishiyama, H.; Saito, N.; Yashima, T.; Sato, K.; Inoue, Y. *Surf. Sci.* **1999**, *427/428*, 152.
(7) Saito, N.; Ohkawara, Y.; Sato, K.; Inoue, Y. *MRS Symp. Proc.* **1998**, *497*, 215.
(8) Ohkawara, Y.; Saito, N.; Inoue, Y. *Chem. Phys. Lett.* **1998**, *286*, 502.
(9) Saito, N.; Inoue, Y. *J. Chem. Phys.* **2000**, *113*, 469.
(10) Saito, N.; Nishiyama, H.; Sato, K.; Inoue, Y. *Surf. Sci.* **2000**, *454/456*, 1099.
(11) Saito, N.; Nishiyama, H.; Inoue, Y. *Appl. Surf. Sci.* **2001**, *169/170*, 259.
(12) Inoue, Y. *Catalysis Survey from Japan* **1999**, *3*, 95.
(13) Saito, N.; Nishiyama, H.; Sato, K.; Inoue, Y. *Chem. Phys. Lett.* **1998**, *297*, 72.
(14) Saito, N.; Sato, K.; Inoue, Y. *Surf. Sci.* **1998**, *417*, 384.
(15) Saito, N.; Sakamoto, M.; Nishiyama, H.; Inoue, Y. *Chem Phys. Lett.* **2001**, *341*, 232.
(16) Ikeda, T. *Fundamentals of Piezoelectricity*; Oxford University Press: New York, 1990; p 117
(17) Auld, B. A. *Acoustic Fields and Waves in Solids*; Wiley & Sons: New York, 1973; Vol 2.
(18) Lang, N. D.; Kohn, W. *Phys. Rev.* **1970**, *B1*, 4555.
(19) Smith, J. R. *Phys. Rev.* **1969**, *181*, 522.
(20) Marcel, R. I. *Principles of Adsorption and Reactions on Solid Surfaces*; Wiley & Sons: New York, 1996.
(21) Somorjai, G. *Introduction to Surface Chemistry and Catalysis*; Wiley & Sons: New York, 1994.
(22) Kratochwil, Th.; Wittmann, M.; Küppers, J. *J. Electron Spectrosc. Relat. Phenom.* **1993**, *64/65*, 609.